ADVANCED ENERGY MATERIALS
www.advenergymat.de

First-Cycle Oxidative Generation of Lithium Nucleation Sites Stabilizes Lithium-Metal Electrodes

*Yu-Kai Huang, Ruijun Pan, David Rehnlund, Zhaohui Wang, and Leif Nyholm**

Although lithium-metal electrodes have very high capacities, their use as negative electrodes in batteries is associated with stability and safety problems due to formation of dendrites, mossy as well as dead lithium. These problems generally result from the difficulty to ensure that the deposition and stripping of lithium occur homogeneously on the entire electrode surface. As a result, the lithium-metal electrode is gradually transformed into a thick, porous, and poorly performing electrode. It is therefore essential to develop approaches that facilitate the attainment of homogeneous (i.e., 2D) lithium nucleation and growth. It is also important to note that if the lithium electrode is oxidized on the first half-cycle, the formed oxidation pits will control the subsequent lithium deposition step. Herein, it is shown that the performance of lithium-metal electrodes can be straightforwardly improved by introducing a short (e.g., 1 s long) potentiostatic pulse so that the first oxidation step takes place more homogeneously on the lithium surface. This surface activation step gives rise to a large number of preferential lithium nucleation sites facilitating the subsequent attainment of a uniform lithium deposition step. The experimental results indicate that this straightforward pulse approach can significantly increase the lifetime of lithium-metal electrodes.

1. Introduction

With a high theoretic specific capacity of 3860 mAh g^{-1} and a low standard potential of −3.04 V versus the standard hydrogen electrode, the lithium-metal electrode (LME) has been regarded as the "Holy Grail" in connection with the realization of high-energy-density lithium batteries.[1,2] However, LMEs are generally prone to side reactions with the electrolyte as well as the formation of lithium dendrites, mossy lithium, and pits during the lithium deposition and stripping (i.e., oxidation) steps, respectively. This is particularly true in conventional ethylene carbonate (EC) based electrolytes typically containing 1 M of a lithium salt such as $LiPF_6$.[3–6] This incidentally means that such electrolytes are good test systems when developing new approaches to circumvent the abovementioned problems. One important reason for this behavior is that 3D rather than 2D lithium deposition is obtained under such experimental conditions.[7] As the LMEs become more and more porous, the performances of the LMEs degrade resulting in short battery life-times. To circumvent this, many materials- and chemistry-related strategies involving, for example, conductive porous hosts, artificial solid electrolyte interphase layers, and modified electrolytes, have been proposed to stabilize LMEs.[8,9] However, few researchers have addressed the LME problems from a more fundamental electrochemical point-of view by, for example, considering the likelihood of obtaining the required 2D nucleation and growth of lithium in conventional electrolytes. This is somewhat surprising given that the electrodeposition of metals has been discussed in detail within the electrochemical community.[10,11] It is, for example, known that the attainment of 2D nucleation and growth of the deposits requires the application of a sufficiently large overpotential to form a high nuclei density on the electrode surface since the nuclei density depends strongly on the overpotential. Although the positive correlation between the nuclei density and applied current density (and thus the overpotential) has been shown for the deposition of lithium on copper electrodes in an ether-based electrolyte,[12] the deposition conditions are significantly different when depositing lithium on an LME using conventional EC-based electrolytes. As explained by Rehnlund et al.,[7] it should in fact be very difficult to obtain true 2D deposition and growth of lithium on an LME in a conventional 1 M $LiPF_6$ electrolytes

Y.-K. Huang, Dr. Z. Wang, Prof. L. Nyholm
Department of Chemistry–Ångström Laboratory
Uppsala University
Box 538, Uppsala SE-751 21, Sweden
E-mail: Leif.Nyholm@kemi.uu.se

Dr. R. Pan
Materials Science and Engineering Program and Texas Materials Institute
The University of Texas at Austin
Austin, TX 78712, USA

Dr. D. Rehnlund
Institute for Applied Biosciences
Department of Applied Biology
Karlsruhe Institute of Technology
Fritz-Haber-Weg 2, Karlsruhe 76131, Germany

Dr. Z. Wang
College of Materials Science and Engineering
Hunan University
Changsha 410082, China

The ORCID identification number(s) for the author(s) of this article can be found under https://doi.org/10.1002/aenm.202003674.

DOI: 10.1002/aenm.202003674

as only a few nuclei are likely to form during the deposition step. This is a result of the fact that the potential of the LME always should be close to its equilibrium potential (i.e., 0 V versus Li^+/Li) in such an electrolyte. Nevertheless, Rehnlund et al.,[7] demonstrated that 2D nucleation and growth of lithium still can be obtained on the entire LME surface by decreasing the $LiPF_6$ concentration to 0.020 M and applying a 10 ms long potentiostatic deposition pulse during the nucleation on the first cycle. In this way, a high overpotential and hence a multitude of homogeneously distributed nuclei could be obtained, and the nuclei were then allowed to grow under normal galvanostatic current conditions. This nucleation pulse approach was, on the other hand, not that effective in a conventional 1 M $LiPF_6$ electrolyte since the LME then functions as an almost ideal nonpolarisable electrode. It is therefore clear that other approaches are needed to obtain 2D nucleation and growth of lithium on LMEs in conventional 1 M $LiPF_6$ electrolytes.

One possible approach could be to electrochemically generate a large number of very similar nucleation sites on the LME during a lithium stripping step prior to the first deposition step. The idea here is that these sites then would serve as preferential nucleation sites during the subsequent lithium deposition step. At this point, it should be noted that while most researchers have approached the LME stability problems by trying to improve the performance of the lithium deposition step directly, it is well-known that the lithium deposition step is affected by the preceding lithium stripping step.[7,13–15] Despite this, only a few studies have so far focused on the importance of the preceding lithium stripping step.[13–16] This situation is difficult to understand, particularly when aiming at the development of lithium-metal batteries (LMBs) containing lithium-free positive electrodes, as the first step would involve stripping lithium from the LME rather than lithium deposition. As this stripping step generates the surface on which the subsequent lithium deposition step will take place, it is clearly important to be able to control the first lithium stripping step. Liu et al.[14] demonstrated that an LME, first subjected to a galvanostatic stripping step, performed quite differently compared to an LME first subjected to a galvanostatic deposition step. The inclusion of a preceding galvanostatic stripping step resulted in the formation of large and deep pits that were not homogenously distributed at the lithium surface. Those pits then served as preferential nucleation sites resulting in an uneven deposition of lithium and a higher overall resistance. Sanchez et al.[15] recently demonstrated that the "nucleation" density of dendrites and pits depended on the current density and that the formation of dead lithium mainly was controlled by the "nucleation" step (i.e., the initial stage of forming dendrites and pits). Based on these findings and the results described by Rehnlund et al.,[7] one would expect that a much more homogeneous lithium deposition could be obtained if a short potentiostatic stripping pulse were to be used to generate a multitude of similarly-sized and homogeneously-distributed pits prior to the subsequent conventional galvanostatic deposition step. Another important question is if such a potentiostatic stripping pulse-based approach would enable 2D lithium nucleation and growth in a conventional 1 M $LiPF_6$ electrolyte. While it appears unlikely based on the findings of Rehnlund et al,[7] we are not aware of any previous attempts of using a stripping pulse on the first cycle as the first step to improve the performance of LMEs.

Herein, we describe an LME activation approach in which a potentiostatic stripping pulse is included to activate the LME prior to the first deposition step by intentionally forming a multitude of pits which then facilitate the formation of more homogeneous lithium deposits (see **Figure 1**). The fundamental idea is that relatively few pits are formed (only at the most electrochemically active sites) during the stripping step under normal constant-current cycling conditions.[5,7,14,15] To circumvent this "active site" problem, a potentiostatic pulse is applied prior to the conventional galvanostatic stripping step on the first cycle to ensure that the stripping process takes place more uniformly at the entire electrode surface. As the generated pits act as subsequent nucleation sites, a more homogeneous deposition of lithium should be obtained, which should result in improved stability and thus longer lifetime of the LME. It should be noted that the proposed strategy is fundamentally different from the so-called pulse charging/discharging approach in which a "galvanostatic" pulse and a pause are alternatively applied throughout the cycling and/or simulated cycling.[17,18] The pulse charging/discharging approach, which does not involve the use of an activation or nucleation pulse that is only used on the first cycle, has in fact been shown not being able to provide 2D lithium nucleation in the absence of a nucleation pulse.[7] The results presented here, on the other hand, clearly show that the stripping pulse on the first cycle significantly improves the subsequent performance of LMEs in very good agreement with the hypothesis described above.

2. Results and Discussion

As explained above, this work aims at exploring the possibilities of obtaining 2D lithium deposition and growth on LMEs via the generation of a multitude of homogeneously distributed nucleation sites after the first galvanostatic stripping step with the aid of a potentiostatic stripping pulse. Stripping of lithium hence always preceded lithium deposition as would be the case when using an LME in combination with a lithium-free positive electrode. The experiments were performed with three-electrode lithium cells (containing three LMEs) and conventional LP40 electrolyte (i.e., 1 M $LiPF_6$ in EC: diethyl carbonate (DEC) = 1:1 (v/v) without any additive), using galvanostatic cycling with a current density and a stripping/deposition charge of 1.0 mA cm^{-2} and 1.0 mAh cm^{-2}, respectively. The three-electrode setup allowed the application of potentiostatic pulses to the working electrode as well as the recording of the individual potential profiles (i.e., chronopotentiograms) for both the working and counter electrodes. Conventional LP40 electrolyte, containing no additive, was chosen as a test electrolyte as LMEs are known to perform particularly poorly in EC-based electrolytes.[7,15,19] The use of this electrolyte should hence facilitate a fundamental evaluation of the efficiency of the present approach. As electrolytes consisting of $LiPF_6$ dissolved in EC-based solvent mixtures are the dominant type of electrolytes in conjunction with lithium-based battery technologies/industries, it would clearly also be very valuable if the LME performance in LP40 could be significantly improved using the present approach. As the electrochemical results (i.e., chronopotentiograms) are relatively insensitive

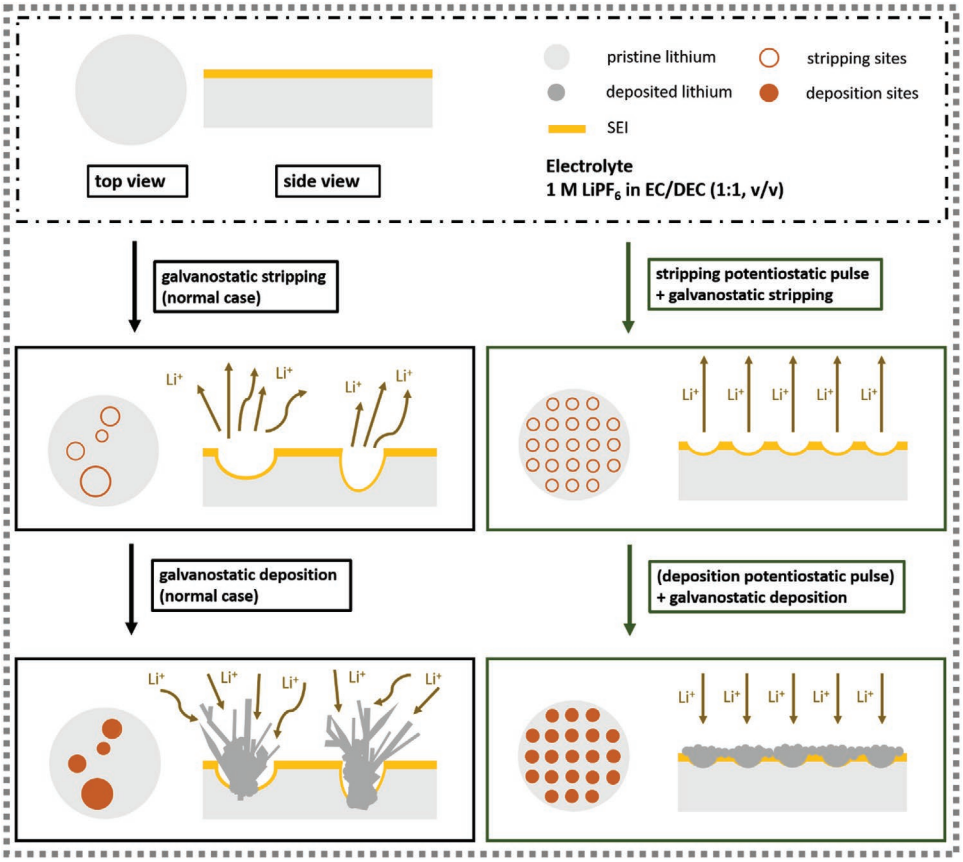

Figure 1. The potentiostatic stripping-pulse approach in conventional LP40 electrolyte (i.e., 1 M $LiPF_6$ in EC:DEC = 1:1 (v/v)).

to changes in the surface morphology of the electrodes,[7] the effects of the stripping pulses will mainly be evaluated based on the comparisons of the electrode surface morphologies analyzed with scanning electron microscopy (SEM). A transfer box was used to make sure that the lithium samples were not exposed to air when transported from the glovebox to the SEM instrument.

First, experiments were designed to find a suitable pulse height and duration of the potentiostatic stripping pulse. A series of experiments with different pulse heights were therefore conducted to identify the value required to obtain a multitude of equally sized pits (i.e., nucleation sites) homogeneously distributed on the electrode surface after the first galvanostatic stripping step. Here it should be recalled that, in this work, the lithium stripping always preceded the lithium deposition so that the first stripping step served as an activation step with respect to the first deposition step. In **Figures 2** and **3**, SEM images depicting the LME surface after the first galvanostatic stripping step in the absence and presence of a preceding 1 s-long potentiostatic stripping pulse with various pulse heights are compared. In these experiments, a 100 ms long pause was included between the potentiostatic stripping pulse and the galvanostatic stripping step to allow the generated Li^+ concentration profile at the electrode surface to relax.[7,20] Variations of the surface concentration of Li^+ were previously shown to be able to significantly affect the nucleation and growth of lithium on LMEs.[7] As shown in Figure 2a–c, the use of small pulse heights (e.g., 0.05 or 0.1 V) did not give rise to a more homogeneous distribution of pits on the electrode surface. This suggests that the 0.05 and 0.1 V pulses only caused stripping to take place at sites that were originally more electrochemically active. Those pulses, in fact, lead to an even more non-uniform stripping since the stripping reaction then becomes confined to a few sites on the electrode surface. When the applied pulse height was increased further, the pit density increased, and the pit distribution also became more uniform (see Figure 2d–f). The results from the digital image analyses based on the SEM images (Figures 2d–f and 3a) showed that the average size of the pits became smaller and that the number of pits increased when a larger pulse height was employed (See Figure 2g–j). This is in very good agreement with the hypothesis that a potentiostatic stripping pulse with a large pulse height should activate an increased fraction of the electrode surface.

As is evident from Figure 3 the inclusion of a potentiostatic stripping pulse with a pulse height of 4 V and duration of 1 s prior to the galvanostatic stripping step was found to yield an even more homogeneous distribution of pits on the lithium surface (compare Figure 3a,c). In this case, shallower and interconnected "depressions" were observed, most likely formed via the merging of a number of small pits (see Figure 3d). In this case, it was, however, not possible to carry out the same image analysis as no completely discrete pits could be identified in the SEM images. This indicates that the 4 V potentiostatic stripping pulse gave rise to a more uniform and more 2D stripping behavior

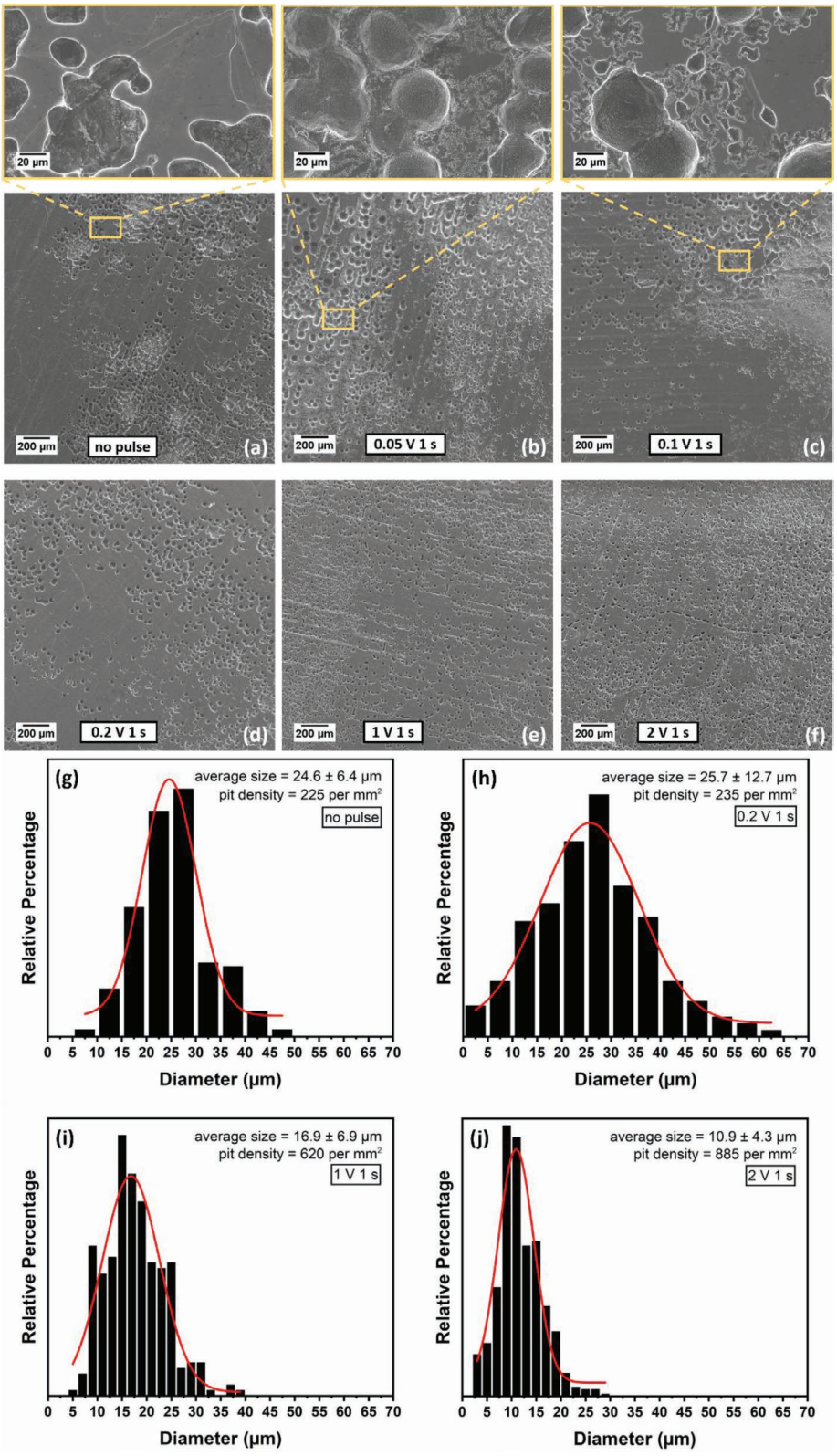

Figure 2. (Upper panel) SEM images depicting the LME surface after the first galvanostatic stripping step a) in the absence, and presence of a preceding 1 s-long potentiostatic stripping pulse with a pulse height of b) 0.05 V, c) 0.1 V, d) 0.2, e) 1 V, and f) 2 V, respectively. The top images in (a–c) show magnifications of the indicated regions. The constant current density and charge used in the galvanostatic stripping step were 1.0 mA cm^{-2} and 1.0 mAh cm^{-2}, respectively. (Lower panel) The pit size distribution and pit areal density derived from digital image analyses based on g) Figure 3a, h) Figure 2d, i) Figure 2e, and j) Figure 2f.

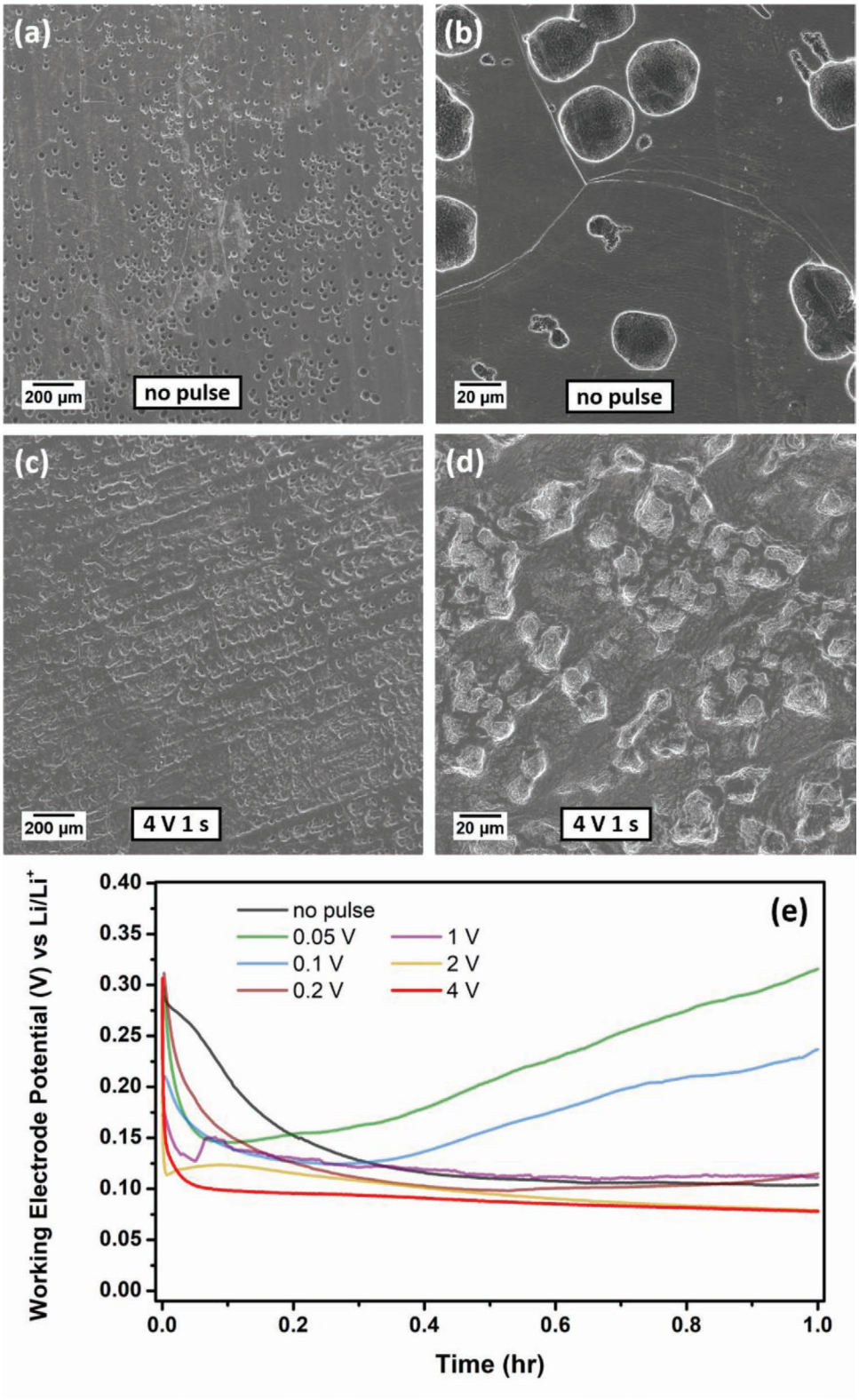

Figure 3. (Upper panel) SEM images of the LME surface at different magnifications after the first galvanostatic stripping step. The (a) and (b) images were obtained in the absence of a potentiostatic stripping pulse whereas the (c) and (d) images were obtained with a preceding potentiostatic stripping pulse with a pulse height of 4 V and duration of 1 s. (Lower panel) e) chronopotentiograms depicting the first galvanostatic stripping steps in the presence and absence of different preceding potentiostatic stripping pulses. The constant current density and charge for the galvanostatic stripping step were 1.0 mA cm^{-2} and 1.0 mAh cm^{-2}, respectively.

across the lithium surface during the subsequent galvanostatic stripping step. This is also in good agreement with the electrochemical results as the chronopotentiogram in this case featured a significant potential change in the beginning of the galvanostatic stripping step followed by a rather steady potential during the rest period of the stripping step (see Figure 3e). Without the stripping pulse, no such steady-state potential was reached, and the potential decayed with time, indicating that the growth of the relatively large pits gave rise to an increasing electroactive surface area and hence a lower overpotential. For a sufficiently low pulse height (e.g., 0.05 or 0.1 V), there was, on the other hand, an increase in the potential during most of the stripping step period indicating an increasing overpotential. The increase suggests that new pits had to be formed to enable the stripping reaction to support the applied current (see Figure 3e and the magnified regions in Figure 2b,c). The results in Figure 3 clearly demonstrate that comparisons of SEM images are very valuable complements to analyses of the shapes of the chronopotentiograms. One problem with the interpretation of the chronopotentiograms is that the electrochemical performance reflects the performance of the entire electrode surface. This means that the appearance of local features may not be readily visible due to their relatively small contributions to the surface area. This is in good agreement with previous findings involving lithium electrodeposition on LMEs.[7]

The results discussed above thus imply that the LME surface can be viewed as a surface containing a range of sites with different electrochemical activities, in analogy with the models used in conjunction with the electrodeposition of metals.[10,11] Under normal galvanostatic conditions, the stripping should only take place at the most active sites yielding only a few but large pits.[15] When a preceding potentiostatic stripping pulse with an increasing pulse height is used, more and more sites become electrochemically active. As a result, the subsequent galvanostatic stripping step would involve many more sites on the electrode surface, which leads to a large number of small and more homogeneously distributed pits. Assuming that the homogeneously distributed pits act as preferential lithium nucleation sites, the use of such a potentiostatic stripping step should consequently facilitate the attainment of uniform and 2D deposition of lithium.

Experiments were also conducted to study the effects of the stripping pulse duration on the size and distributions of the obtained pits after the subsequent galvanostatic stripping step. A less homogeneous distribution of pits was obtained when the pulse duration of the 4 V pulse was shortened to 10 or 200 ms (compare Figure S1, Supporting Information and Figure 3c). This indicates that the formation of the pits required some time (see below) even when using a 4 V pulse, suggesting that the resulting overpotential was too low due to the abovementioned redox buffering capacity of the LME (see the Introduction Section). If a sufficiently high overpotential could have been reached, a shorter pulse time than 1 s would most likely have been sufficient. In a 1 M $LiPF_6$ electrolyte, it is, however, difficult to adopt larger pulse heights than 4 V due to the large currents produced. The experiments with different pulse heights and pulse durations, nevertheless, suggest that a preceding potentiostatic stripping pulse of 4 V for 1 s was able to decrease the influence of the active site problem and provide a homogeneous distribution of pits after the subsequent galvanostatic stripping step.

To acquire more insight regarding the influence of the stripping pulse, the morphologies of the LME surfaces were also studied directly after the application of different potentiostatic stripping pulses (see **Figure 4**). When the pulse height was increased to 4 V, a large number of homogeneously distributed long and tiny pits with dimensions of a few microns were observed (see Figure 4a–d). The observed structure most likely stemmed from the intrinsic nano-/micro-structured morphology on the lithium foil surface generated during the lithium processing process as previously explained.[7] Here it should also be noted that the oxidation charge generated during the 1 s long stripping pulse of 4 V was merely around 0.04 mAh (or 0.026 mAh cm^{-2}) whereas that of the galvanostatic stripping step was 1.54 mAh (or 1.0 mAh cm^{-2}). This oxidation charge difference explains the larger pits seen in, for example, Figures 3c,d. In Figure 4d–g, on the other hand, a series of SEM images show the development of the tiny pits at different periods of time during the 4 V stripping pulse. The images reveal that the formation of the tiny pits was progressive rather than instantaneous (i.e., that new pits were gradually formed and developed during the stripping pulse). This supports the hypothesis that the overpotential imposed by the 4 V pulse was too low to instantaneously activate all sites. The reason for this is that it should be very difficult to polarize an LME immersed in a 1 M $LiPF_6$ electrolyte due to its high inherent redox buffer capacity. Besides, it should be pointed out that the potential of the working electrode reached during the potentiostatic pulse was much lower than 4 V due to the presence of a large iR drop. Nevertheless, by comparing the results in Figure 4 with the surface morphologies obtained after the subsequent galvanostatic stripping in Figures 2 and 3 and Figure S1, Supporting Information, the effects of a stripping pulse with a pulse height of 4 V and a duration of 1 s can clearly be seen. It can be concluded that the stripping pulse of 4 V for 1 s resulted in the formation of homogeneously distributed and well-developed tiny pits which allowed the following galvanostatic stripping to be better controlled. As shown in Figure 3 this approach gave rise to a more homogeneous stripping result.

To further characterize the activated surfaces, electrochemical impedance spectroscopy (EIS) experiments were carried out using a frequency range from 100 kHz to 1 Hz and an ac potential amplitude of 10 mV in three-electrode lithium cells. These experiments were carried out before and after the potentiostatic stripping pulse (i.e., 4 V for 1 s), and after the first stripping step with and without the preceding stripping pulse (see **Figure 5**). From the results, presented in the form of Nyquist plot in Figure 5a, it is clear that the applied potentiostatic stripping pulse decreased the charge transfer resistance associated with the lithium working electrode. This change could be correlated with the features seen in the SEM images in Figure 4d. The stripping pulse generated a large number of homogeneously distributed tiny pits on the surface of the LME, which electrochemically activated the LME surface and thus decreased the charge transfer resistance via a decrease in the current density. The EIS data are also in excellent agreement with the chronopotentiograms recorded during the first galvanostatic stripping step in Figure 3e. With the application

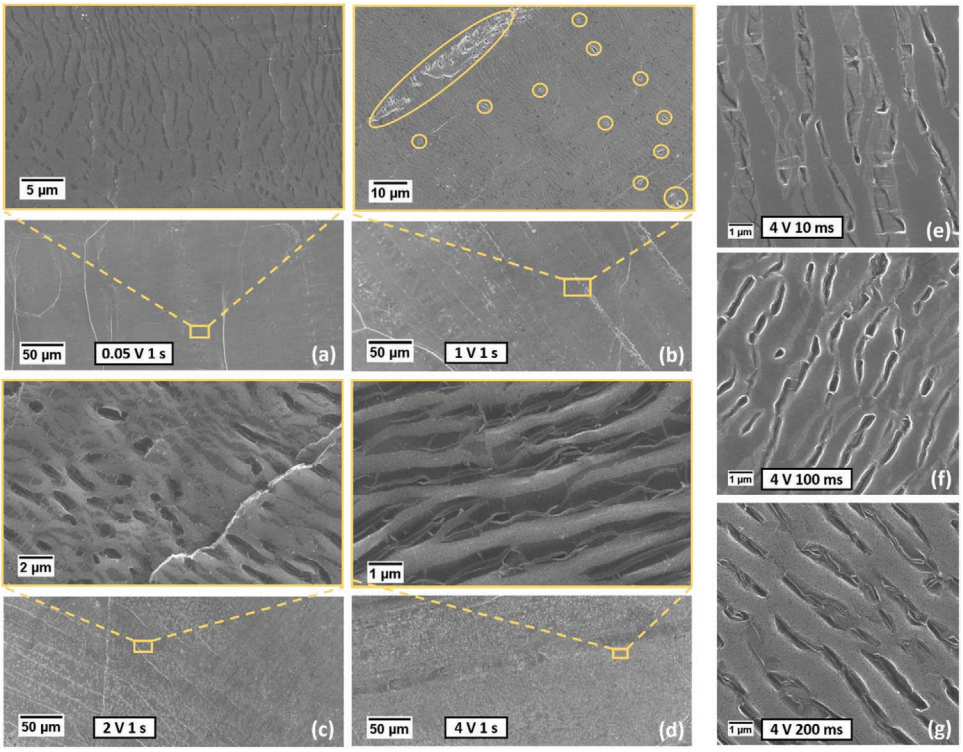

Figure 4. SEM images of the LME surface obtained after applying only a potentiostatic stripping pulse with a pulse height and duration of a) 0.05 V for 1 s, b) 1 V for 1 s, c) 2 V for 1 s, d) 4 V for 1 s, e) 4 V for 10 ms, f) 4 V for 100 ms, and g) 4 V for 200 ms, respectively. The top images in the (a–d) cases show magnifications of the indicated regions. Tiny pits started to form when the pulse height reached 1 V as indicated in the magnification of the (b) image.

of the stripping pulse, the lithium stripping was able to take place more homogeneously across the surface, which resulted in the potential reaching a relatively constant value within short time. A much larger charge transfer resistance was consequently seen before applying the stripping pulse (i.e., in pristine state), as the lithium stripping only involved some "active sites" at the LME surface (see Figure 5a). This gave rise to a preferential growth of the active pits, which can explain the gradually increasing potential seen in the chronopotentiogram as well as the surface morphologies in Figure 3. The Nyquist plots acquired after the first galvanostatic stripping step with and without the stripping pulse are compared in Figure 5b. A smaller charge transfer resistance was evidently seen in the presence of the stripping pulse in excellent agreement with the results discussed above. In the absence of the stripping pulse, a "shoulder" in the high frequency range can also be seen in Figure 5b suggesting the presence of another semicircle and hence a less homogeneous surface as well as less well-defined stripping process.[21] These EIS results consequently support the hypothesis that a stripping pulse can be used to activate

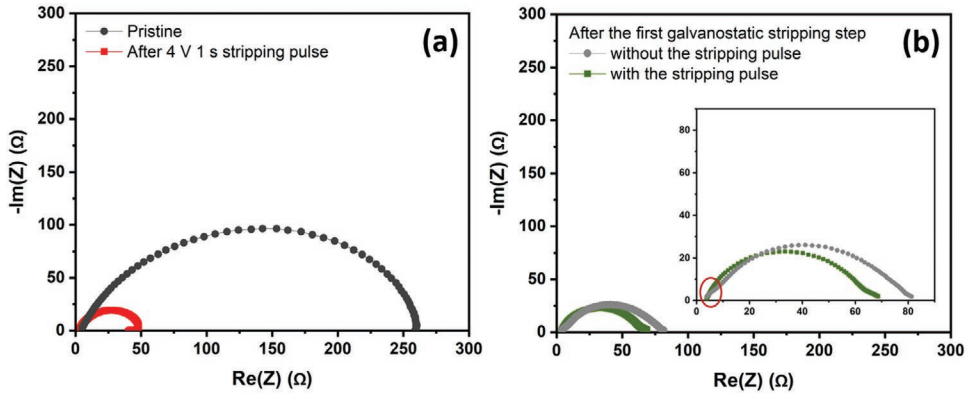

Figure 5. Electrochemical impedance data, presented as Nyquist plots, for the lithium working electrodes a) before and after the use of a 4 V potentiostatic stripping pulse with a duration of 1 s, and b) after the first galvanostatic stripping step with and without the preceding stripping pulse (i.e., 4 V for 1 s). The inserted figure in (b) shows the magnified plots in which the high-frequency shoulder is indicated. The frequency range was 100 kHz to 1 Hz and the constant current density and charge used in the galvanostatic stripping step were 1.0 mA cm^{-2} and 1.0 mAh cm^{-2}, respectively.

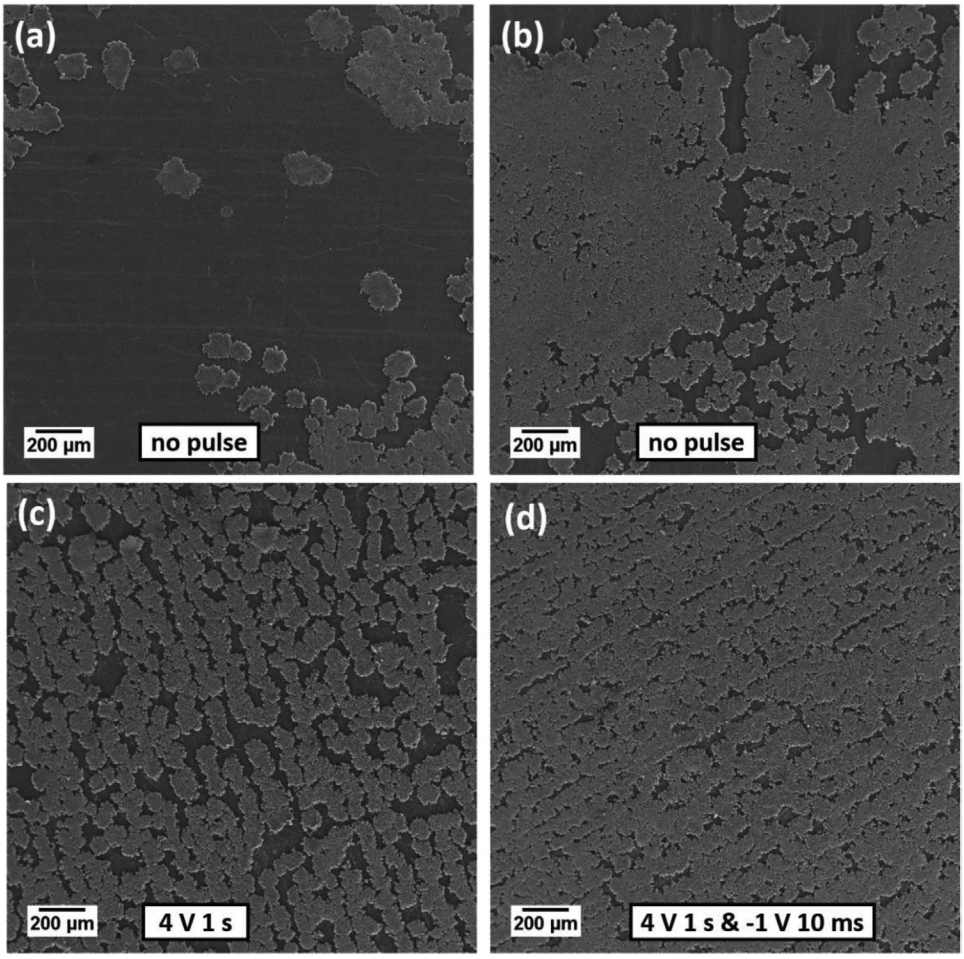

Figure 6. SEM images depicting the LME surface after the first galvanostatic lithium deposition step preceded by the first galvanostatic stripping step in (a) and (b) the absence, and c) the presence of the potentiostatic stripping pulse (4 V for 1 s) prior to the galvanostatic stripping step. Note that the (a) and (b) images depict two different regions. The image in (d) shows the result obtained in the presence of the potentiostatic stripping pulse (4 V for 1 s) prior to the first galvanostatic stripping step with a deposition potentiostatic pulse (–1 V for 10 ms) included prior to the galvanostatic deposition step. The constant current density and charge for the galvanostatic stripping and deposition steps were 1.0 mA cm^{-2} and 1.0 mAh cm^{-2}, respectively. The employed experimental conditions are summarized in Table S1, Supporting Information.

the electrode surface via the generation of an increased electrochemically active area. This is in excellent agreement with the results in Figure 3 and the strategy outlined in Figure 1. Since the stripping behavior is known to affect the subsequent lithium deposition behavior,[7,13] it is reasonable to assume that the present approach should facilitate the attainment of 2D lithium deposition via the generation of a large number of similar nucleation sites.

Experiments were consequently carried out to investigate how the performances of the LMEs were affected by the above-mentioned oxidative activation step. The surface morphologies of the LMEs after the subsequent galvanostatic deposition step were studied employing the experimental conditions presented in Table S1, Supporting Information. As seen in **Figure 6** homogeneously distributed lithium deposits were obtained when the 4 V stripping pulse was used prior to the first galvanostatic stripping step. In the absence of the stripping pulse, lithium was, on the other hand, only deposited in some regions (see Figure 6a,b). This behavior is in excellent agreement with the hypothesis that only a limited number of nuclei are formed under conventional cycling conditions and that an oxidative generation of a large number of pits, subsequently acting as preferential lithium nucleation sites, can facilitate the attainment of 2D lithium deposition. Besides, an even better result was obtained by including a potentiostatic deposition pulse (–1 V for 10 ms) prior to the galvanostatic deposition step (see Figure 6d). As mentioned in the introduction, such a deposition pulse was previously shown to be able to increase the lithium nucleation density,[7] thus yielding a more homogeneous deposition. The main difference in the electrochemical performances with and without the stripping and deposition pulses was seen during the first galvanostatic stripping step (see Figure 3e and Figure S1c, Supporting Information as well as **Figure 7**a). This suggests that the more homogeneous deposits seen in Figure 6c,d (compared with Figure 6a,b) mainly resulted from the potentiostatic stripping pulse as the pulse facilitated the formation of homogeneous nucleation sites. Here it should be mentioned that there are several studies demonstrating the possibility of

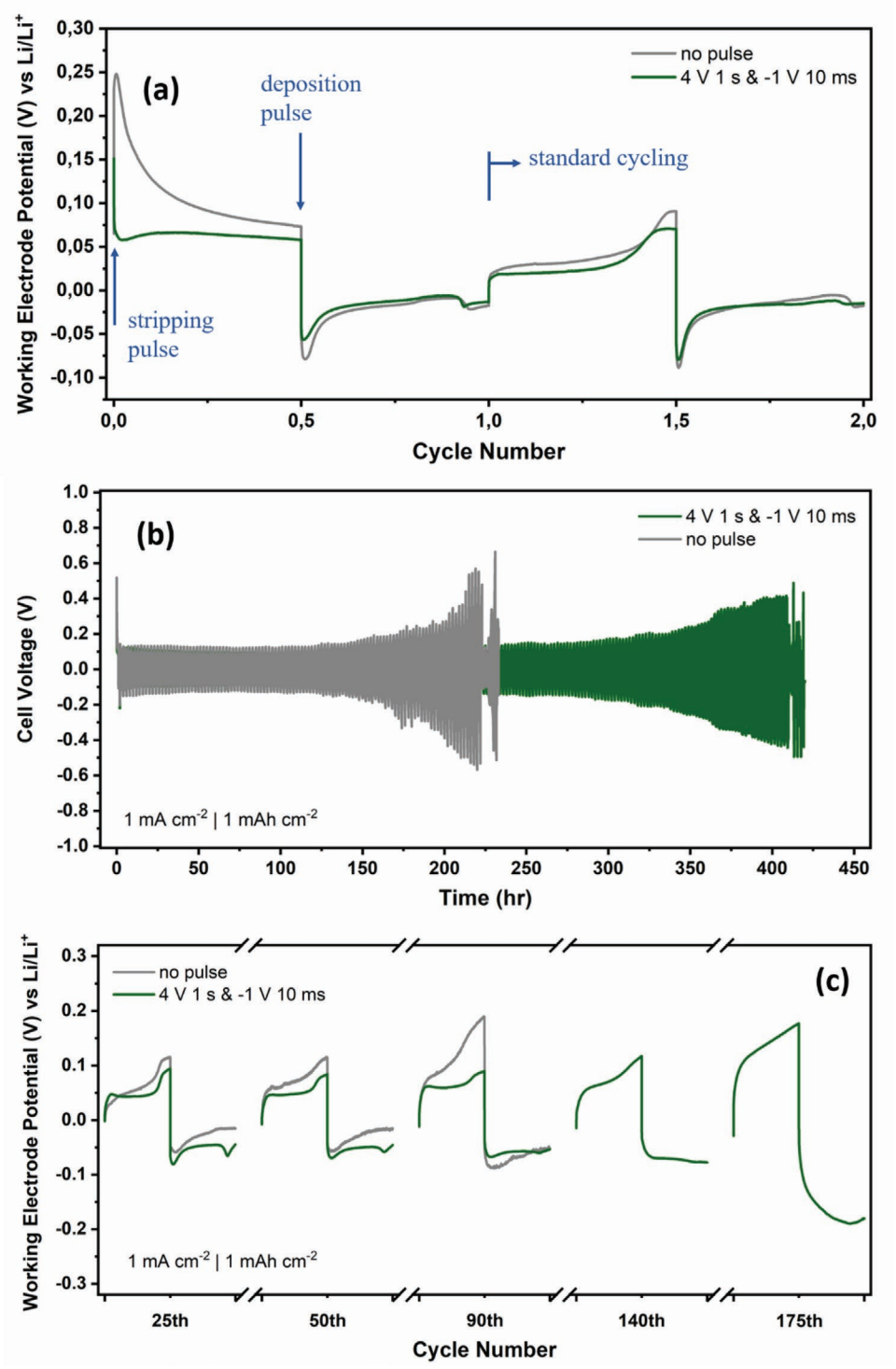

Figure 7. Galvanostatic charge and discharge curves (chronopotentiograms) for three-electrode lithium cells showing a) the first two cycles in the presence and absence of a potentiostatic stripping pulse (4 V for 1 s) and a deposition pulse (–1 V for 10 ms) on the first cycle, b) the long-time cycling performances of the abovementioned cells, and c) the chronopotentiograms for the lithium working electrodes at the indicated cycle numbers. All galvanostatic stripping and deposition steps were carried out with a constant current density of 1.0 mA cm^{-2} and a capacity of 1.0 mAh cm^{-2}.

achieving similar effects by mechanically introducing ordered patterns/pits onto the electrode surface before cycling.[22–24] While those ordered patterns were also reported to be able to guide the lithium deposition, this concept is fundamentally different compared to the present stripping pulse approach. The ex situ mechanical method is in fact more related to manufacturing 3D host structures to accommodate lithium deposits, whereas the present in situ stripping pulse approach focuses on

obtaining a homogeneous activation of entire electrode surface and thus controlling the subsequent stripping and deposition behaviors, especially during the nucleation steps. It is likewise important to note that deposits with different morphologies were obtained even though the shapes of the chronopotentiograms for the first galvanostatic deposition step were found to be similar with and without the stripping and deposition pulses (See Figure 7a). This demonstrates the importance of employing SEM images in lithium deposition and stripping studies. A higher initial potential (i.e., a larger overpotential for the nucleation) was, however, seen in the absence of the pulses due to fewer nucleation sites in good agreement with the EIS data in Figure 5b. As LMEs perform poorly in LP40-like electrolytes whereas better performances have been found in ether-based electrolytes,[25] experiments were also carried out in cells containing an ether-based electrolyte (i.e., 1 M lithium bis(trifluoromethanesulfonyl)imide (LiTFSI) in 1,3-dioxolane (DOL): 1,2-dimethoxyethane (DME) = 1:1 (v/v)), see the Experimental Section) to further evaluate the applicability of the proposed approach. The preliminary results show that the inclusions of the potentiostatic pulses can improve the results also in the 1 M LiTFSI ether-based electrolyte, as can be seen in Figure S2, Supporting Information depicting the surface morphologies of the LMEs after the first cycle with and without the pulses, respectively. While more work clearly is needed to investigate the applicability of the present pulse approach to different types of electrolytes, such activities are beyond the scope of the present study focusing on proof-of principle investigations in a LP40 electrolyte. It should, however, also be noted that the electrochemical stability windows of ether-based electrolytes with a lithium salt concentration close to 1 M can be problematic in combination with a high-voltage cathode material.[2] Improving the performances of LMEs in LP40-like electrolytes is therefore still highly relevant to the development of high-voltage LMBs.

Although the results discussed above indicate that the first-cycle performance of the LME can be significantly improved with the stripping pulse approach, the performance of the LME clearly also needs to be tested during many stripping and deposition cycles. Here, it should be pointed out that the stripping and deposition pulses were only used on the first cycle (i.e., prior to the first stripping and deposition steps, respectively). The reason for this is that the morphology obtained on the first cycle should serve as a template during the subsequent cycles. Previous findings have also shown that the inclusion of a nucleation pulse on each cycle resulted in the formation of less homogeneous lithium deposits instead.[7] In Figure S3, Supporting Information, SEM images of the electrode surface, obtained after the second cycle galvanostatic stripping and deposition steps, respectively, are shown. More homogeneous lithium deposits were again found when the potentiostatic stripping and deposition pulses were used (see Figure S3f,g, Supporting Information). Inactive regions could still be seen after two cycles of conventional galvanostatic cycling (see Figure S3e, Supporting Information) demonstrating the intrinsic non-uniformity of the lithium stripping and deposition due to the "active site" problem. Approaches that result in a more homogeneous and 2D nucleation and growth of lithium are hence clearly needed to improve the cycle lives of LMEs. However, on the second cycle where standard galvanostatic cycling was carried out, the electrochemical performances were rather similar regardless of whether stripping and deposition pulses were used on the first cycle or not (see Figure 7a).

A closer look at the results in Figure S3, Supporting Information, however, shows that some deposited lithium remained on the electrode surface after the second stripping step (see Figure S3a–d, Supporting Information), even when the deposition and stripping experiments were carried out with a constant deposition and stripping charge of 1.0 mAh cm^{-2}. This means that there were new pits been formed during the stripping step. While newly formed pits were observed on the electrode surface in the absence of the stripping and deposition pulses on the first cycle (see Figure S3a,b, Supporting Information), no such pit formation could be detected in the presence of these pulses (see Figure S3c,d, Supporting Information). Although the formation of new pits is suggested by the increase in the potential toward the end of the second stripping step in Figure 7a in both cases, the potential was lower with the pulses.[25] This shows that the electrode surface was activated in a more homogeneous way after the first stripping step due to the inclusion of the stripping pulse. The lithium left at the electrode surface can be explained by the presence of dead lithium, formed as a result of the inability to completely oxidize the deposited lithium during the subsequent galvanostatic stripping step.[26,27] Although the stripping pulse approach can improve the results significantly, the SEM images in Figure S3c,d, Supporting Information hence still show that the formation of dead lithium could not be completely avoided in LP40 electrolyte. This is, however, not surprising as true 2D deposition and stripping of lithium are very difficult to obtain in LP40 electrolyte.[7,19] If the lithium deposition step is not truly 2D, the subsequent cycling will result in the formation of more and more mossy and dendritic lithium as well as dead lithium. As mentioned before, the high redox buffer capacity of an LME immersed in a 1 M $LiPF_6$ electrolyte (e.g., LP40 electrolyte) makes it difficult to reach the sufficiently high overpotentials needed to obtain 2D lithium nucleation and growth. A large overpotential should analogously be required to ensure that the stripping of lithium takes place all over the electrode surface. However, in LP40 electrolyte, only very small overpotentials are needed for an LME to provide a large oxidation or reduction current, which is incidentally the reason why LMEs are used in half-cells when testing other electrode materials. The inability to eliminate the formation of dead lithium in LP40 electrolyte can thus be explained by the difficulty to form pits and to nucleate lithium truly all over the electrode surface as sufficiently large overpotentials cannot be reached during the stripping and deposition pulses. This hypothesis is supported by recent findings indicating that it is possible to obtain 2D lithium deposition by decreasing the $LiPF_6$ concentration from 1.0 M to, for example, 20 mM as mentioned in Introduction.[7] The decreased $LiPF_6$ concentration enabled larger overpotentials to be reached which yielded a much higher nuclei density across the electrode surface during the deposition pulse. The present work was carried out to investigate if an oxidative generation of preferential nucleation sites could be used as an alternative to a decreased $LiPF_6$ concentration. As will be described in more detail below, this does unfortunately not appear to be the case.

The long-time cycling performances of three-electrode lithium cells which were cycled with and without the stripping

and deposition pulses on the first cycle are compared in Figure 7b. It is immediately clear that the inclusion of the pulses on the first cycle resulted in a significantly increased lifetime of the cell. The practical cell failure, defined as when the absolute cell voltage exceeds 0.3 V,[5] hence occurred after 182 and 102 cycles for the cells with and without the pulses, respectively. These results clearly show that while the pulse approach increases the lifetime of the cell, it is not able to solve the fundamental problem, in good agreement with the results discussed above.

A comparison of the first two galvanostatic stripping steps in Figure 7a in fact suggests that new pits were already formed during the second stripping step as discussed above. This indicates that true 2D lithium deposition was not obtained even during the first deposition step possibly due to the nucleation issues in 1 M $LiPF_6$ electrolyte discussed above (see Figure S4, Supporting Information). While lower overpotentials were seen during the deposition steps when adopting the pulse approach, the differences were less pronounced than for the corresponding stripping steps, at least initially (See Figure 7a). During the first deposition step, an overpotential was first seen after which the absolute value of the potential gradually decreased. This suggests a growth of the formed nuclei resulting in a larger electroactive area and hence a lower current density. Toward the end of the deposition step, the overpotential, however, increased again suggesting the onset of another type of deposition (e.g., a more 3D deposition) both with and without the pulses. The results also suggest that this type of nucleation behavior was coupled to the increase in the stripping potential seen on the subsequent cycle, implying that the second type of deposition facilitated the formation of dead lithium.

The long-term effects of the first-cycle pulses can be more clearly seen in Figure 7c which shows chronopotentiograms for the lithium working electrodes at different cycle numbers. It can be seen that the working electrode potential during the galvanostatic stripping step was maintained lower for many more cycles (see, e.g., the 90th cycle curves) with little increase in the overpotential when the pulse approach was adopted. This indicates that the oxidation of the deposited lithium was more well-defined in the case with the pulses. This is most likely because the lithium was deposited more homogeneously on the electrode surface, thus less dead lithium was formed during the subsequent stripping step. Even though the results show that new pits were formed in both cases as discussed above, the influence of this effect was smaller in the presence of the pulses. The fact that the degree of increase in the potential toward the end of the stripping step also depended on the cycle number (see Figure 7c) indicates that the lithium working electrodes, nevertheless, became more and more porous during the cycling. In the absence of the potentiostatic pulses on the first cycle, the overpotential increased faster, especially for the lithium stripping step, which is in good agreement with the results from the initial cycles seen in Figure S3, Supporting Information and Figure 7a. The higher overpotentials in fact indicate that the Coulombic efficiencies were lower in the absence of the potentiostatic pulses. Here it should be noted that it is intrinsically difficult to calculate the Coulombic efficiencies for lithium symmetric cells, particularly under the present experimental conditions involving a fixed current and capacity for the galvanostatic steps.[28] It is reasonable to assume that the improved performance seen when using the first-cycle pulses was due to the initial generation of a more homogeneous distribution of pits. This activated the LME as the pits then served as preferential nucleation sites during the subsequent lithium deposition step. The results in Figure 7 thus demonstrate that it is very important to start off with an LME surface that has been properly activated to reduce the "active site" effect so that the likelihood of obtaining 2D lithium deposition is increased. If this is not the case, the performance of the electrode degrades more quickly as the electrode is converted faster into a more and more porous electrode composed of mossy and dendritic lithium which results in dead lithium, an increased cell impedance, and eventually cell failure.[15,27,29] As true 2D stripping and deposition were not achieved even with the pulses, it must, however, also be concluded that the pulse approach merely can extend the life-time of the LME in LP40 electrolyte. This is, however, not surprising as previous findings indicate that it should be difficult to obtain 2D stripping and deposition in a 1 M $LiPF_6$ electrolyte due to the problems associated with the activation of the entire electrode surface.[7] One possibility could be to use a electrolyte with lower Li^+ concentration as this would enable the attainment of larger overpotentials during the pulses and thus facilitate true 2D stripping and deposition. Another, more straightforward, approach would be to combine the present pulse approach with other approaches found to prolong the lifetime of LMEs.

3. Conclusion

The constant-current cycling performance of an LME can be significantly increased by including a short oxidative potentiostatic pulse before the first galvanostatic stripping step on the first cycle to electrochemically activate the electrode surface via the formation of a homogeneous distribution of small pits. Those pits then can act as preferential nucleation sites during the subsequent lithium deposition. To facilitate 2D lithium nucleation and growth, a short potentiostatic deposition pulse can likewise be used prior to the first galvanostatic deposition step. The present in situ electrochemical strategy which is used to control the lithium stripping and deposition behaviors on the first cycle to improve those in the subsequent (pulse-free) cycles was demonstrated using a potentiostatic stripping pulse with an amplitude of 4 V and a duration of 1 s as well as a 10 ms deposition pulse with an amplitude of –1 V. The electrochemical activation approach resulted in decreased overpotentials for the galvanostatic lithium stripping and deposition steps, indicating a decreased formation of mossy and dead lithium which yielded a longer LME lifetime. The present approach is particularly important when an LME is first subjected to stripping with the subsequent lithium deposition involving the generated pits. The performance of the LME should, in this case, depend on the first stripping step which would generate the pits used on the subsequent cycles. It is also concluded that it is difficult to obtain true 2D lithium deposition and growth in a LP40 electrolyte even with the abovementioned pulse approach. It can be explained by the high redox buffer capacity of an LME immersed in a 1 M $LiPF_6$ electrolyte as this effect makes

it difficult to attain the high overpotentials required to obtain a homogeneous formation of pits as well as lithium nuclei during the stripping and deposition steps, respectively. Nevertheless, the present pulse approach can still readily be used in combination with other approaches to obtain even better functioning LMEs for Li-metal and Li-sulfur batteries.

4. Experimental Section

Materials: The lithium foil (125 µm, Cyprus Foote Minerals) and Celgard 2400 monolayer polypropylene separator (25 µm, Celgard Co.) were purchased from the indicated companies. The lithium foil was punched into pieces with a diameter of 14 mm (i.e., with an area of 1.54 cm^{-2}). The Celgard 2400 separators were cut into discs with a diameter of 20 mm which were dried in a Buchi glass oven at 70 °C for 5 h in a glovebox to remove residual moisture prior to the cell assembly. Unless stated otherwise, the electrolyte used in the experiments was LP40 (i.e., 1 M $LiPF_6$ in EC:DEC = 1:1 (v/v) without any additive), purchased from Solvionic and used as received. As discussed in the Results and Discussion Section, some experiments were also carried out with an ether-based electrolyte prepared by dissolving lithium bis(trifluoromethanesulfonyl)imide (LiTFSI, BASF) in a solvent mixture of 1,3-dioxolane (DOL, anhydrous, 99.8%, Sigma Aldrich) and 1,2-dimethoxyethane (DME, Selectilyte, BASF), yielding 1 M LiTFSI in DOL/DME = 1:1 (v/v). The LiTFSI salt was first dried in a Buchi glass oven at 120 °C for 48 h to remove residual moisture before usage. All preparations were conducted in a glovebox under an argon atmosphere with oxygen and water contents lower than 1 ppm.

Cell Assembly: The stripping and deposition experiments were carried out with lithium symmetric pouch cells using a three-electrode setup in which two pieces of the punched lithium foils were employed as the working and counter electrode, respectively, while a third rectangular piece of lithium foil was used as a reference electrode. The reference electrode was separated from the working and counter electrodes using two Celgard separators soaked with 40 µL electrolyte. The separators were larger than the lithium working and counter electrodes, so the reference electrode would not block the path between the two electrodes. As two separators were used the total separator thickness was 50 µm while the total amount of electrolyte was 80 µL. The same procedure was used for the cells containing the LP40 and the 1 M LiTFSI ether-based electrolytes. The cell assembly was done in a glovebox under an argon atmosphere with oxygen and water contents lower than 1 ppm.

Electrochemical Experiments: All electrochemical experiments were conducted using a multichannel potentiostat/galvanostat (VMP-2, Biologic). In the series of stripping experiments, a potentiostatic stripping pulse with different pulse heights (i.e., 0.05, 0.1, 0.2, 1, 2, and 4 V) and duration (i.e., 10, 100, 200, and 1000 ms) was used. After the stripping pulse, a 100 ms long pause was applied prior to the galvanostatic stripping step to allow the concentration profile generated by the stripping pulse to relax. The galvanostatic stripping step was performed with a current density of 1.0 mA cm^{-2} (i.e., a current of 1.54 mA) and a total charge of 1.0 mAh cm^{-2} (i.e., 5.54 C). In the subsequent deposition experiment, a deposition (nucleation) pulse of −1 V was applied for 10 ms, after which a 100 ms pause was employed (to allow relaxation of the concentration profile) prior to the galvanostatic deposition step. The galvanostatic deposition step was also carried out with a current density of 1.0 mA cm^{-2} (i.e., 1.54 mA) and a total charge of 1.0 mAh cm^{-2} (i.e., 5.54 C). On the second cycle and subsequent cycles, no pulses were used and standard galvanostatic cycling was hence carried out with the same current density of 1.0 mA cm^{-2} and total charge of 1.0 mAh cm^{-2}. For comparison, experiments were also carried out without the stripping and deposition pulses. EIS was carried out with a frequency range from 100 kHz to 1 Hz and an amplitude of 10 mV using three-electrode lithium cells before and after the application of a potentiostatic pulse (4 V for 1 s) followed by a 100 ms long pause to mimic the situation right before the galvanostatic stripping step in the stripping experiments. Another set of EIS experiments was also conducted in the symmetric cells with the same frequency range but after the first galvanostatic stripping step with and without the stripping pulse and measurements were conducted after a 10-min pause after the galvanostatic stripping step.

Long-Time Galvanostatic Cycling: The long-time galvanostatic cycling experiments were performed using the VMP-2 potentiostat/galvanostat to test the long-time cycling performance and lifetime of the three-electrode lithium cells described above. In these experiments, the cells were cycled using a constant current density of 1.0 mA cm^{-2} (i.e., 1.54 mA) and a total stripping and deposition charge of 1.0 mAh cm^{-2} (i.e., 5.54 C), with or without the application of potentiostatic stripping and deposition pulses on the first cycle.

Characterizations: The surfaces of the LMEs were studied using high resolution SEM (Merlin, Zeiss). After a stripping and/or deposition experiment, the pouch cell was transferred back into a glovebox for disassembly. The lithium foil that had served as the working electrode was then retrieved and washed several times with dimethyl carbonate. The lithium foil was then dried before being placed on a stage in a transfer device (Semilab) which then was closed in the glovebox and hence filled with argon gas. As a result of this, the lithium samples were transported to the SEM instrument without being exposed to air. The analyses of the pit size distribution and pit density based on the SEM images were carried out in ImageJ software according to the following steps: 1) coloring the pits with black color, 2) picking up the pits with "Threshold" function, and 3) using "Analyze Particles" function to get the total number of the pits and their individual areas. The pits were assumed to have circular shapes and their diameters were calculated from the areas of the pits. Finally, a Gaussian function was used to obtain the statistics summaries of the data.

Supporting Information

Supporting Information is available from the Wiley Online Library or from the author.

Acknowledgements

Dr. Maria Paschalidou is acknowledged for her assistance with the SEM experiments. Financial support from the Swedish Research Council (VR-2017-06320 and VR-2019-04276), The Ångström Advanced Battery Center, and StandUp are also gratefully acknowledged.

Conflict of Interest

The authors declare no conflict of interest.

Data Availability Statement

Data openly available in a public repository that issues datasets with DOIs.

Keywords

2D, dendrites, lithium-metal electrodes, nucleation and growth, oxidation pulses

Received: November 25, 2020
Revised: January 3, 2021
Published online:

[1] G. N. Lewis, F. G. Keyes, *J. Am. Chem. Soc.* **1913**, *35*, 340.
[2] M. Winter, B. Barnett, K. Xu, *Chem. Rev.* **2018**, *118*, 11433.
[3] X. Q. Zhang, X. B. Cheng, Q. Zhang, *Adv. Mater. Interfaces* **2018**, *5*, 1701097.
[4] Y. S. Cohen, Y. Cohen, D. Aurbach, *J. Phys. Chem. B* **2000**, *104*, 12282.
[5] K. N. Wood, M. Noked, N. P. Dasgupta, *ACS Energy Lett.* **2017**, *2*, 664.
[6] S. Li, M. Jiang, Y. Xie, H. Xu, J. Jia, J. Li, *Adv. Mater.* **2018**, *30*, 1706375.
[7] D. Rehnlund, C. Ihrfors, J. Maibach, L. Nyholm, *Mater. Today* **2018**, *21*, 1010.
[8] X. B. Cheng, R. Zhang, C. Z. Zhao, Q. Zhang, *Chem. Rev.* **2017**, *117*, 10403.
[9] Y. Zhang, T. T. Zuo, J. Popovic, K. Lim, Y. X. Yin, J. Maier, Y. G. Guo, *Mater. Today* **2020**, *33*, 56.
[10] R. Greff, R. Peat, L. M. Peter, D. Pletcher, J. Robinson, *Instrumental Methods in Electrochemistry*, Ellis Horwood, Hemel Hempsted **1990**.
[11] M. Paunovic, M. Schlesinger, *Fundamentals of Electrochemical Deposition*, Wiley, New York **1998**.
[12] A. Pei, G. Zheng, F. Shi, Y. Li, Y. Cui, *Nano Lett.* **2017**, *17*, 1132.
[13] L. Gireaud, S. Grugeon, S. Laruelle, B. Yrieix, J. M. Tarascon, *Electrochem. Commun.* **2006**, *8*, 1639.
[14] H. Liu, X. Cheng, R. Xu, X. Zhang, C. Yan, J. Huang, *Adv. Energy Mater.* **2019**, *9*, 1902254.
[15] A. J. Sanchez, E. Kazyak, Y. Chen, K. H. Chen, E. R. Pattison, N. P. Dasgupta, *ACS Energy Lett.* **2020**, *5*, 994.
[16] F. Shi, A. Pei, D. T. Boyle, J. Xie, X. Yu, X. Zhang, Y. Cui, *Proc. Natl. Acad. Sci. USA* **2018**, *115*, 8529.
[17] Q. Li, S. Tan, L. Li, Y. Lu, Y. He, *Sci. Adv.* **2017**, *3*, e1701246.
[18] A. Aryanfar, D. Brooks, B. V. Merinov, W. A. Goddard, A. J. Colussi, M. R. Hoffmann, *J. Phys. Chem. Lett.* **2014**, *5*, 1721.
[19] R. Pan, X. Xu, R. Sun, Z. Wang, J. Lindh, K. Edström, M. Strømme, L. Nyholm, *Small* **2018**, *14*, 1704371.
[20] M. S. Chandrasekar, M. Pushpavanam, *Electrochim. Acta* **2008**, *53*, 3313.
[21] J. Fleig, J. Maier, *J. Electroceram.* **1997**, *1*, 73.
[22] Q. Li, B. Quan, W. Li, J. Lu, J. Zheng, X. Yu, J. Li, H. Li, *Nano Energy* **2018**, *45*, 463.
[23] M. H. Ryou, Y. M. Lee, Y. Lee, M. Winter, P. Bieker, *Adv. Funct. Mater.* **2015**, *25*, 834.
[24] J. Park, J. Jeong, Y. Lee, M. Oh, M. H. Ryou, Y. M. Lee, *Adv. Mater. Interfaces* **2016**, *3*, 1600140.
[25] K. N. Wood, E. Kazyak, A. F. Chadwick, K. H. Chen, J. G. Zhang, K. Thornton, N. P. Dasgupta, *ACS Cent. Sci.* **2016**, *2*, 790.
[26] C. Fang, J. Li, M. Zhang, Y. Zhang, F. Yang, J. Z. Lee, M. H. Lee, J. Alvarado, M. A. Schroeder, Y. Yang, B. Lu, N. Williams, M. Ceja, L. Yang, M. Cai, J. Gu, K. Xu, X. Wang, Y. S. Meng, *Nature* **2019**, *572*, 511.
[27] K. H. Chen, K. N. Wood, E. Kazyak, W. S. Lepage, A. L. Davis, A. J. Sanchez, N. P. Dasgupta, *J. Mater. Chem. A* **2017**, *5*, 11671.
[28] B. D. Adams, J. Zheng, X. Ren, W. Xu, J. G. Zhang, *Adv. Energy Mater.* **2018**, *8*, 1702097.
[29] B. Wu, J. Lochala, T. Taverne, J. Xiao, *Nano Energy* **2017**, *40*, 34.